JOURNAL OF MATERIALS SCIENCE 30 (1995) 5723–5731

Interaction between the TiC(TiCN)–Ni–Mo hardmetals and chromium vapours

I. YU. KONYASHIN
Hardmetal Technologies, Zelyony Prospect 67-1-117, Moscow 111399, Russia

The interaction between TiC or TiCN-based hardmetals with a Ni–Mo binder, or cermets, and chromium vapour in a vacuum was investigated over a wide temperature range acceptable for depositing wear-resistant coatings without the formation of a liquid phase in the cermets. Computer modelling in the Ti–C–Cr system showed that a direct interaction of TiC with chromium, leading to the formation of chromium carbides, is not possible because of the high thermodynamic stability of titanium carbide. It was established experimentally that as a result of the interaction between the cermets and chromium vapours, a coating characterized by a two-layer structure was deposited on the cermet surface. The coating consists of an inner layer adjacent to the substrate, which is composed of the chromium and carbon solid solution in nickel, and an outer layer composed of a mixture of $(Cr, Ni)_7C_3$ and $(Cr, Ni)_{23}C_6$. The activation energy of the deposition process is 387 kJ mol^{-1} which is close to the value of the chromium heat of evaporation. The coating deposition process is supposed to be limited by the rate of the external supply of chromium from the vapour phase. The results of the investigation of the structure, composition and morphology of the coating are presented. A mechanism responsible for the interaction of the cermets with chromium vapour leading to the formation of the two-layer coating, is proposed.

1. Introduction

In recent years TiC- or TiCN-based hardmetals, or cermets, have been widely utilized as materials for the manufacture of cutting tools. Although these materials are used instead of coated WC-based hardmetals, a number of attempts to apply conventional chemical (CVD) or physical vapour deposition (PVD) technologies for enhancement of the cermets' wear-resistance have not been successful. At the present time, cermet cutting indexable inserts are usually fabricated without wear-resistant coatings.

Conventional CVD processes for depositing TiC, TiCN, TiN, etc., coatings on the TiC- or TiCN-based cermets with a Ni–Mo binder lead to an unfavourable interaction between the binder and coating during the deposition processes [1–5]. The TiC or TiN coatings deposited on both a nickel underlayer and TiC–Ni–Mo substrate contain a new phase, which is composed of Ti–Ni intermetallics, mainly Ni_3Ti; they crystallize in the form of coarse grains [1]. The coatings are sometimes deposited in the form of dendrites or even needle-like crystals when the hardmetal substrate contains much nickel [2]. Moreover, high porosity is formed under the coatings because of an active incorporation of the binder from the substrate into the coating [3].

The presence of the intermetallic phases in the wear-resistant coatings leads to the appearance of high residual stresses in the coatings when cooling them down after the deposition, because of a substantial difference between thermal expansion coefficients of the coating material and intermetallic phases. The phenomena mentioned above lead to a notable decrease of transverse rupture strength of the coated cermets and the absence of improvement in tool life of the cermets after coating. The unfavourable interaction between the nickel-based binder and the CVD coatings can occur because of both surface or grain-boundary diffusion and the processes of chlorination with subsequent re-deposition of nickel in the volume of the growing coatings. These processes can be depressed or avoided only by the substitution of nickel by cobalt or iron as binding metals [5, 6].

Conventional PVD processes were also used in an attempt to improve performance properties of cermet cutting tools [7–11]. However, in most of these attempts, the deposition of the PVD coatings did not result in substantial improvement in performance properties of the coated cermets. Tool life of the TiN PVD-coated TiC–Ni–Mo cermet did not exceed that of the substrate, because of the formation of a TiNi intermetallic phase at elevated temperatures in turning. The presence of the TiNi phase enhances an interaction between the coated tool and a workpiece which results in worse performance properties of the coated cermets [7]. An unfavourable interaction between a titanium-based high-temperature ionized phase with nickel contained in the cermet substrate, was shown to lead to the formation of a nickel-enriched zone at the substrate–coating interface.

0022–2461

This resulted in poor adhesion of the coating and an insignificant increase of tool life of the coated TiCN–Ni–Mo cermet [11].

Thus, the interaction of cermets with various vapour phases conventionally applied for depositing wear-resistant coatings is very important from the viewpoint of the effectiveness of the coatings for improvement in cermets' tool life. Searching for new compositions of a vapour phase suitable for depositing a single-phase and highly adherent coating well compatible with the cermet substrates, can be a basis for the development of new highly effective technologies for depositing the coatings.

Chromium, carbides of which are applied as wear-resistant coatings for cutting tools, is the only carbide-forming chemical element that does not form intermetallic compounds with nickel and has unlimited intersolubility with it. Furthermore, chromium being vaporized in a vacuum has an elevated vapour pressure, which is high enough for depositing protective coatings due to an interaction with the substrate at temperatures acceptable for coating cermets without the formation of a liquid phase.

The aim of this study was to investigate the process of the interaction between the chromium vapour phase and cermet substrates as well as the composition and structure of the coating deposited on cermets in this way.

2. Experimental procedure

Computer modelling in the Ti–C–Cr system was carried out using the *Universal Program for Defining Equilibrium Parameters in Multicomponental Heterogeneous Systems* [12]. The program includes the informational fund containing data on thermodynamic constants of different substances and a set of programs for calculating the equilibrium composition of various chemical reacting systems. The equilibrium in a closed chemical system of known elemental composition is defined by two variable parameters irrespective of the number of phases, components and chemical reactions. The two of the six parameters can be predetermined: pressure, temperature, volume, entropy, enthalpy and internal energy, as parameters of the equilibrium. The other four parameters, as well as the equilibrium composition of the chemical mixture, can be calculated at a fixed temperature and pressure by means of predetermining the other two parameters as well as an initial composition of the system. Calculating the equilibrium concentrations of chemical mixtures was performed by searching the extremum of the Gibbs free energy value.

Commercially available cermets of the TiCN–Ni–Mo system of the KNT16 grade and of the TiC–Ni–Mo system of the TN20 grade, the composition and source of supply of which are shown in Table I, were utilized for the study of their interaction with chromium vapour. Special model TiCN–Ni–Mo specimens containing 50 wt % Ni were utilized for investigation of the mechanism of this interaction.

The study of the interactions between the cermets and chromium vapour leading to deposition of a coating on the cermets' surface was performed by use of a laboratory furnace of the SSHNV type. The cermet specimens were ultrasonically cleaned and then placed at the surface of a chromium disc of about 12 cm diameter and 3 cm thick. The disc was fabricated before by vacuum sintering of a chromium powder of 99.5% purity at a temperature of about 1700 K for 1 h with subsequent grinding. The chromium disc together with the cermet specimens was placed in an alundum crucible; the crucible was then covered with a molybdenum cover and placed in the vacuum furnace. The inner volume of the furnace was evacuated to a residual pressure of no more than 0.133 Pa and the crucible was then heated to a temperature varying from 1370–1520 K for about 15 min with subsequent annealing for different times. Chromium evaporates actively at these temperatures and chromium vapour interacts with the surface of the cermet specimens, which results in the formation of the coating at the surface of the TiC- or TiCN-based cermets. The temperature of the chromium disc, together with the cermet substrates, was measured by a W–Re thermocouple, which was placed near the surface of the chromium disc, with a precision of $\pm$ 5 K. Thus, the temperature of vaporizing chromium was equal to that of the cermet substrates. After annealing, the crucible was rapidly cooled to a temperature of about 1050 K, at which the pressure of the chromium vapour is negligibly low, and then to room temperature. The cermet specimens were carefully weighed before and after annealing.

Composition, morphology and microstructure of the coating obtained by the interaction of the cermets

TABLE I Composition of the constituent parts of the coatings deposited on the KNT16 and TN20 cermets (the concentration of carbon was not measured)

Substrate					Coating				
Grade, source of supply	Composition (wt %)				Layer	Composition (wt %)[a]			
	TiC	TiCN	Ni	Mo		Ti	Cr	Ni	Mo
KNT16, KZTS Ltd	–	74	19.5	6.5	Carbide	1–2	77–92	6–12	1–2
					Interlayer	2–4	18–27	54–75	1–2
TN20 UzKTZM Ltd	80	–	15.0	5.0	Carbide	1–2	80–91	5–9	1–2
					Interlayer	2–3	15–21	66–78	2–3

[a] Depending on the distance from the coating–substrate interface.

with chromium vapour as well as the intermediate zone between the coating and substrate were examined using a Jeol JSM–35CF scanning electron microscope equipped with the LINK unit for electron-probe micro-analysis (EPMA). Because of relatively low precision of the measurement of concentrations of light elements (carbon, nitrogen, etc.), concentrations of only metals in different phases were measured with relatively high precision; the concentration of carbon was only estimated based on the data obtained. The phase composition and texture of the coatings were examined by X-ray analysis using the DRON-2M X-ray difractometer. The texture was examined by the inclination method at a maximum inclination angle of 60 °C. Defining the crystal lattice parameter of the TiCN phase of the cermet substrate after coating was carried out by removing the coating from the substrate surface by means of hand polishing, with subsequent removal of the binder phase at a depth of more than 10 μm by electrolysis etching. The crystal lattice parameter of the TiCN phase in the core of the cermet substrate was measured utilizing a powder (fabricated by milling) of the coated specimen after removal of the surface layer, of about 2 mm in thickness, with subsequent annealing of the powder.

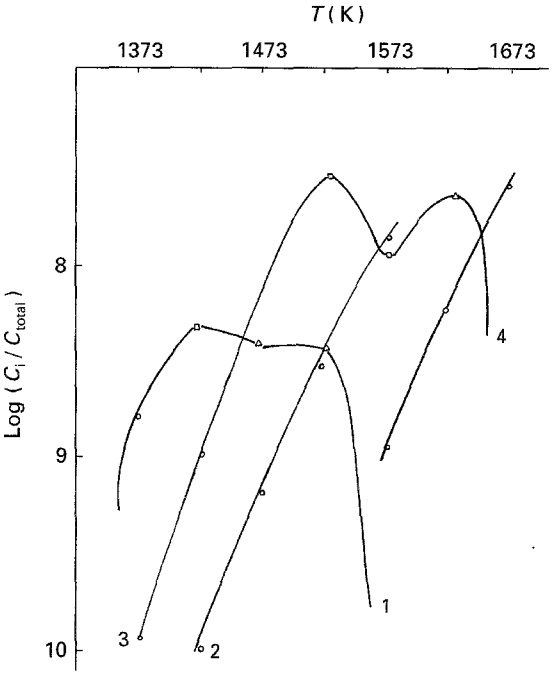

Figure 1 Temperature dependencies of the ratio of the equilibrium amount of chromium carbides to the total amount of chromium at different pressures for the system (wt %) Ti/C/Cr = 1/1/10. (1) 0.133×10^{-1} Pa, (2) 0.133×10^{-2} Pa, (3) 0.133×10^{-3} Pa, (4) 0.133×10^{-4} Pa. (○) $Cr_{23}C_6$, (□) Cr_7C_3, (△) Cr_3C_2.

3. Results and discussion

3.1. Computer modelling in the Ti–Cr–C and Ti–C systems

Carbon diffusion from hardmetal substrates towards a coating takes place usually through a binder phase, which is a solid solution of carbon as well as other elements in cobalt or nickel, and can hardly be modelled by thermodynamic calculations. In spite of this, it seems to be interesting to estimate the thermodynamic potential of the direct interaction between TiC of the cermet substrate and chromium vapour phase. Figs 1 and 2 show results of computer modelling in the Ti–Cr–C and Ti–C systems. The modelling was carried out in a temperature range 1373–1673 K and at values of a residual pressure ranging from 0.133×10^{-1} to 0.133×10^{-4} Pa.

Fig. 1 shows the equilibrium composition of the Ti–Cr–C system; the thermodynamic potential of the formation of chromium carbides is low under the conditions reported here, which is connected with high thermodynamic stability of TiC. Fig. 2 shows that only an insignificant share of carbon is present, not in the form of TiC, but as free or gaseous carbon in the Ti–C system. The results obtained are in agreement with the results of experimental investigations in the TiC–Cr system [13].

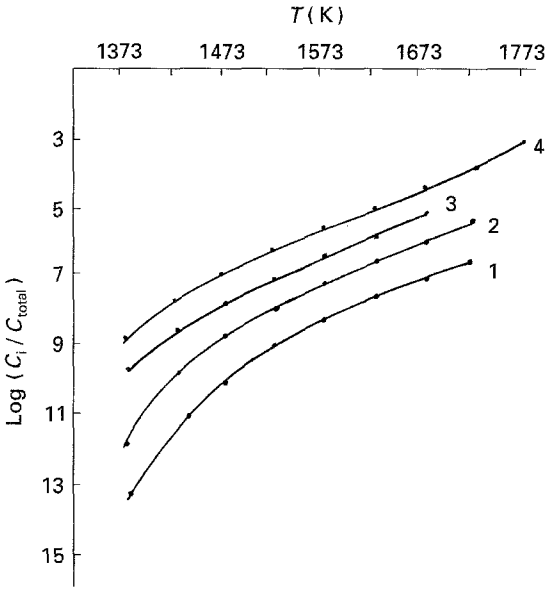

Figure 2 Temperature dependencies of the ratio of the equilibrium amount of gaseous and free carbon to the total amount of carbon at different pressures for the system (wt %) Ti/C = 1/1. (1) 0.133×10^{-1} Pa, (2) 0.133×10^{-2} Pa, (3) 0.133×10^{-3} Pa, (4) 0.133×10^{-4} Pa.

3.2. Kinetics of the interaction between the TiCN cermet and chromium vapour phase

Although the computer modelling reveals the very low thermodynamic potential of the formation of chromium carbides as a result of the direct interaction between TiC and chromium, a carbide coating is formed owing to the interaction between the TiC- or TiCN-based cermets and chromium vapour in a vacuum. Fig. 3 shows the kinetics of the coating process. The curves shown in Fig. 3 reveal that there are two stages during the deposition process. The curves are linear at low temperatures (1370–1450 K); the curve obtained at a temperature of 1470 K has both an initial linear part and a subsequent non-linear one. The kinetic curves have a non-linear character beginning from the temperature of 1500 K, which reveals that the deposition occurs more slowly depending on

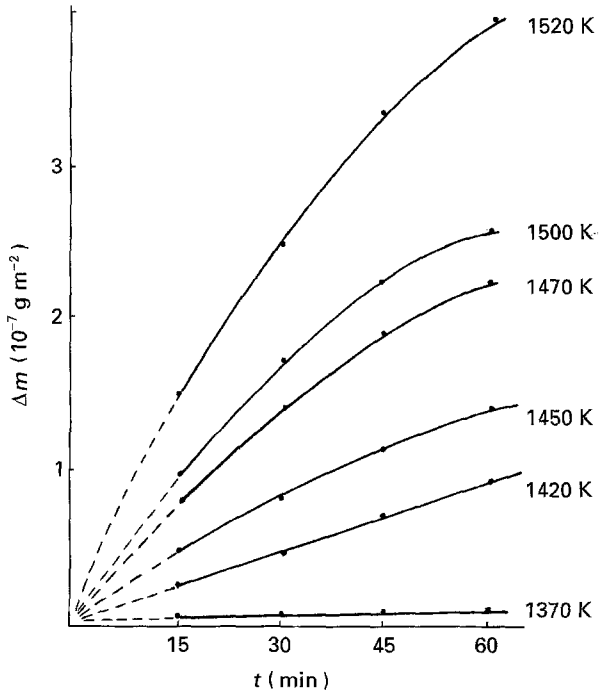

Figure 3 Kinetic curves characterizing the interaction between the KNT16 cermet and chromium vapour at different temperatures.

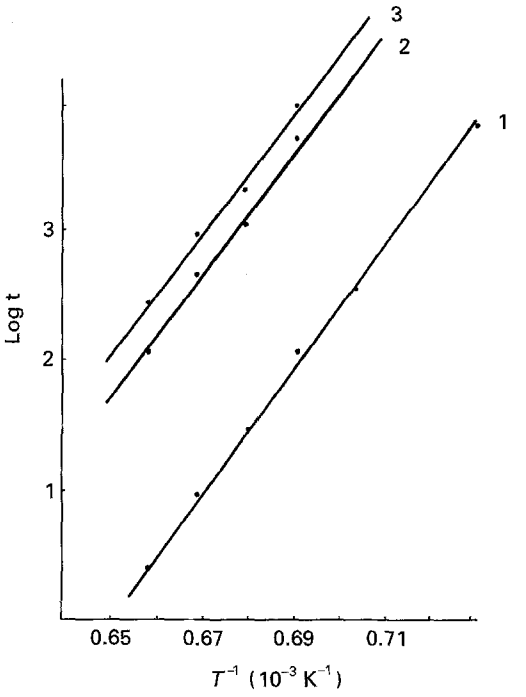

Figure 5 Logarithmic dependencies of the time needed for obtaining the equal specific weight change of the KNT16 cermet specimens versus inverse temperature. The specific weight change is (1) 0.2×10^{-7} g m^{-2}, (2) 1.0×10^{-7} g m^{-2}, (3) 1.2×10^{-7} g m^{-2}.

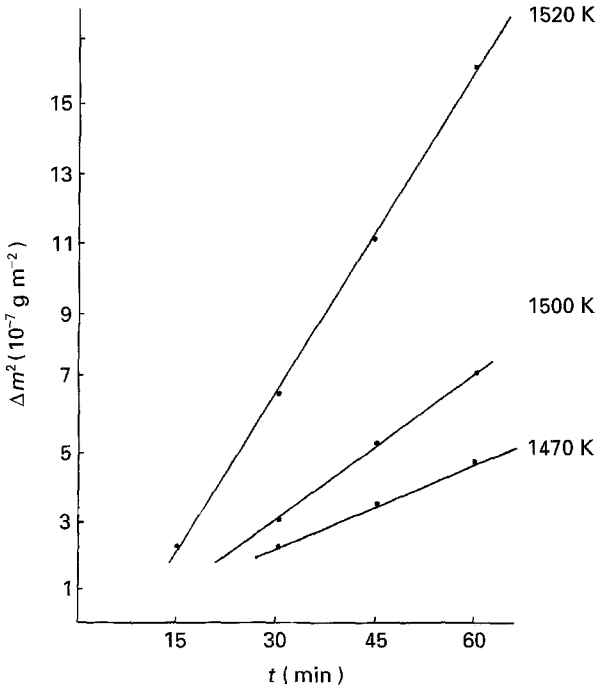

Figure 4 Non-linear sections of the kinetic curves characterizing the deposition of the coating onto the KNT16 cermet re-constructed in the parabolic coordinates.

the process duration. Obviously, the initial stage described by the linear dependence occurs for the short initial period of deposition under these conditions and does not affect the shape of the curves.

The non-linear kinetic curves obtained at temperatures of 1520, 1500 and 1470 K were re-constructed in the coordinates corresponding to the parabolic dependence (Fig. 4). Fig. 4 shows that the curves can be described by the parabolic dependence.

$$\Delta m^2 \sim t \qquad (1)$$

The value of the activation energy was determined by reconstruction of the kinetic curves in the Arrhenius coordinates. The times needed for obtaining equal values of a specific weight change at different temperatures were calculated and are shown in Fig. 5. The curves shown in Fig. 5 are parallel and linear which is evidence of the fact that the limiting stage of the process is not changed in the temperature range investigated. The activation energy value determined is 387 kJ mol^{-1} which is evidence of the fact that the process occurs in the kinetic field. The value of the activation energy obtained is quite high and typical only for some phenomena, like evaporation and sublimation phenomena. The value of chromium heat of evaporation is dependent on temperature; however, it is possible to calculate it's approximate value in a definite temperature range. The chromium heat of evaporation value calculated based on the data of the reference book [14] is approximately equal to 385 kJ mol^{-1} in the temperature range investigated, which is close to the obtained value for the activation energy. The closeness of these two values is supposed to indicate that the limiting stage of the deposition process in the chromium–chromium vapour–coating–substrate system is the chromium evaporation.

It should be mentioned that though the shape of the kinetic curves indicates that the interaction process consists of two stages and the second stage is obviously hampered by the presence of the initially formed coating, the process (as a whole) has the only limiting stage, which is invariable and determined by the chromium evaporation process. This established fact is very important from the viewpoint of possible decarbonization of the cermets' substrate after coating. Carbon diffusion in the substrate is supposedly not a

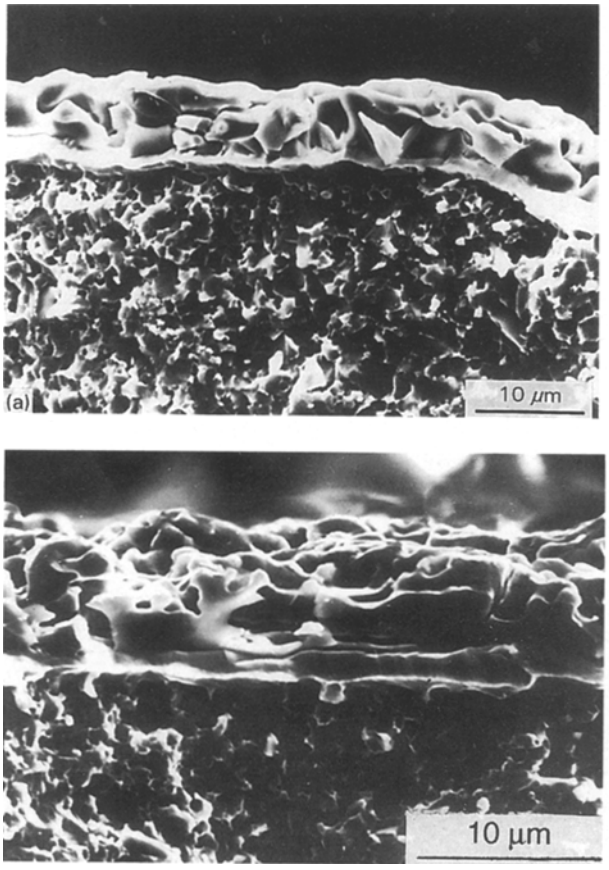

Figure 6 The microstructure of (a) the KNT16 cermet and (b) TN20 cermet with the coating deposited at 1520 K for 1 h.

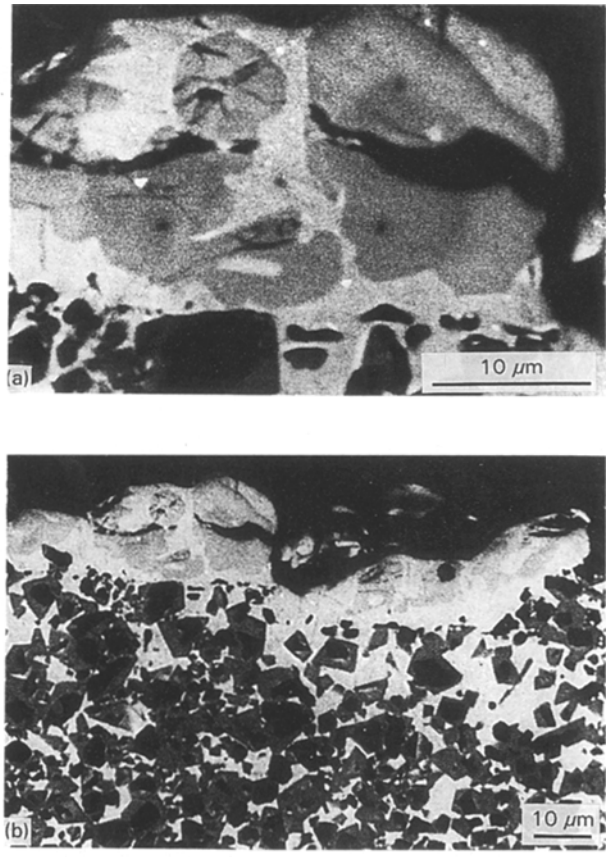

Figure 7 The microstructure of the model alloy containing 50 wt % Ni with the coating deposited at 1520 K for 1 h: (a) the coating (the carbide grains are dark and the binder grains are bright); (b) the substrate with the coating.

limiting stage of the deposition process and the carbide coating formed by the substrate carbon only seems to be deposited without local significant decarbonization of the substrate.

The established two-stage character of the interaction influences the composition and structure of the coatings deposited as a result of this interaction.

3.3. The composition and structure of the coatings

The coatings consist of two layers with a different structure and are formed as a result of the interaction between the TiC(TiCN)–Ni–Mo cermets and chromium vapour phase, which is shown in Fig. 6. The intermediate layer clearly visible in Fig. 6 is up to 2 μm thick and is supposed to be mainly formed during the initial stage of the process when the kinetic curves are linear. The outer layer shown in Fig. 6 is 5–8 μm thick and is probably formed during the second stage of the interaction process when the curves are described by a parabolic dependence.

According to the results of the X-ray analysis and EPMA, which are presented in Table I, the intermediate layer is composed of a solid solution of mainly chromium, as well as titanium and molybdenum, in nickel. This layer is estimated to comprise also up to 5 wt % C. The outer layer is composed of a solid solution of titanium and molybdenum in a mixture of $(Cr, Ni)_7C_3$ and $(Cr, Ni)_{23}C_6$. The carbides possess the axial single-axis textures of (1 0 0) for $(Cr, Ni)_7C_3$ and (1 0 1) for $(Cr, Ni)_{23}C_6$. Results of the EPMA show that chromium diffuses from the coating to the cermet substrates to a depth of more that 100 μm at a temperature of 1520 K for 1 h. The results of the X-ray analysis reveal that there are no Ti–Ni intermetallics, which are formed as a result of significant decarbonization of the TiC(TiCN)–Ni–Mo cermets [15], in the cermets after coating. This is evidence of the fact that there is no local notable decarbonization of the cermet substrates after the formation of the chromium carbide coatings by the substrate carbon only.

Special model specimens with a coarse TiCN phase and a large binder volume were prepared in order to investigate the structure and composition of the coating and intermediate zone. While the KNT16 cermet contains 19.5 wt % Ni, the model alloy contains 50 wt % Ni (Fig. 7). Fig. 8 shows curves characterizing concentrations of different elements in the model alloys under the coating; it is obvious that chromium diffuses to the large volume of the substrate. Table II illustrates the composition of the phases of the model alloy directly under the coating. Most of the chromium penetrates from the coating into the binder phase and the carbonitride phase contains almost no chromium. These data are in agreement with results of the investigation on the crystal lattice period of the carbonitride phase under the coating. While the lattice period of titanium carbonitride in the core is 0.4266 ± 0.0003 nm, that of the carbonitride phase

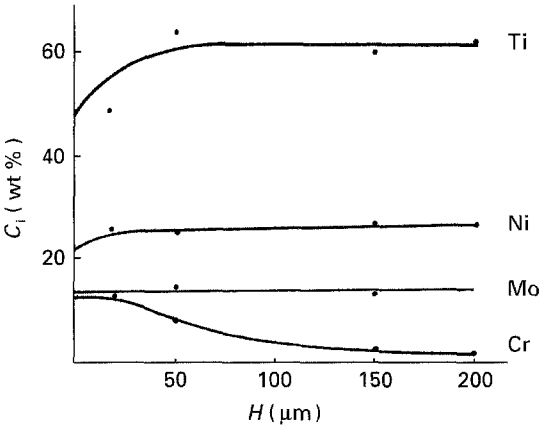

Figure 8 Curves characterizing the distribution of elements in the model alloy containing 50 wt % Ni under the coating deposited at 1520 K for 1 h.

TABLE II Composition of constituent parts of the coating and the substrate for the model alloy containing 50 wt % Ni under the coating (the concentration of carbon was not measured)

Constituent part	Composition (wt %)			
	Ti	Cr	Ni	Mo
Coating, (carbide grain)	0.5	80–81	5–6	12
Coating, (metal matrix)	3	34	57	6
Substrate, TiCN (the core)	99	–	0.6	0.3
Substrate, TiCN (coaxial structure)	78	0.3	1.1	20
Substrate, the binder phase	5	25	62	8

under the coating is 0.4278 ± 0.0003 nm, which is only slightly higher. The insignificant difference between these values can be connected with either some changes in the chemical composition of the TiCN phase after coating or with residual stresses caused by removing the coating from the substrate.

Fig. 7 and Table II show that in the case of the model alloy, the coating is formed not as a two-layer structure but as a structure including the separated chromium carbide grains surrounded by the Ni–Cr matrix. The composition of both phases is close to that of the corresponding layers of the coatings deposited on the KNT16 and TN20 cermets. Although the precision of the measurement of carbon concentration is not high enough, the carbon concentration in the nickel-based matrix of the coating is estimated to range from 3 to 5 wt %. The structure of the coating shown in Fig. 7 is similar to that obtained by liquid-phase sintering of chromium carbide-based hard-metals with a nickel-based binder [16]. This allows the mechanism of the interaction between the cermets and chromium vapour to be interpreted as a liquid-phase one.

3.4. Nucleation and growth of the coatings

Fig. 9a shows a nucleation stage of the deposition. It is apparent that the nickel-based layer is deposited initially as a number of "drops" which are supposed to include a liquid phase. These "drops" then merge together and form a continuous film of the Ni–Cr alloy divided into a number of separate grains (Fig. 9b, c). Fig. 10 shows the Cr–Ni layer crystals formed at different temperatures. It is obvious that the lower is the temperature, the finer is the microstructure of the crystals.

Fig. 11 shows the morphology of the chromium carbide layer at different stages of the deposition process. Initially, the carbide crystals are obviously formed at the surface of the grain boundaries of the

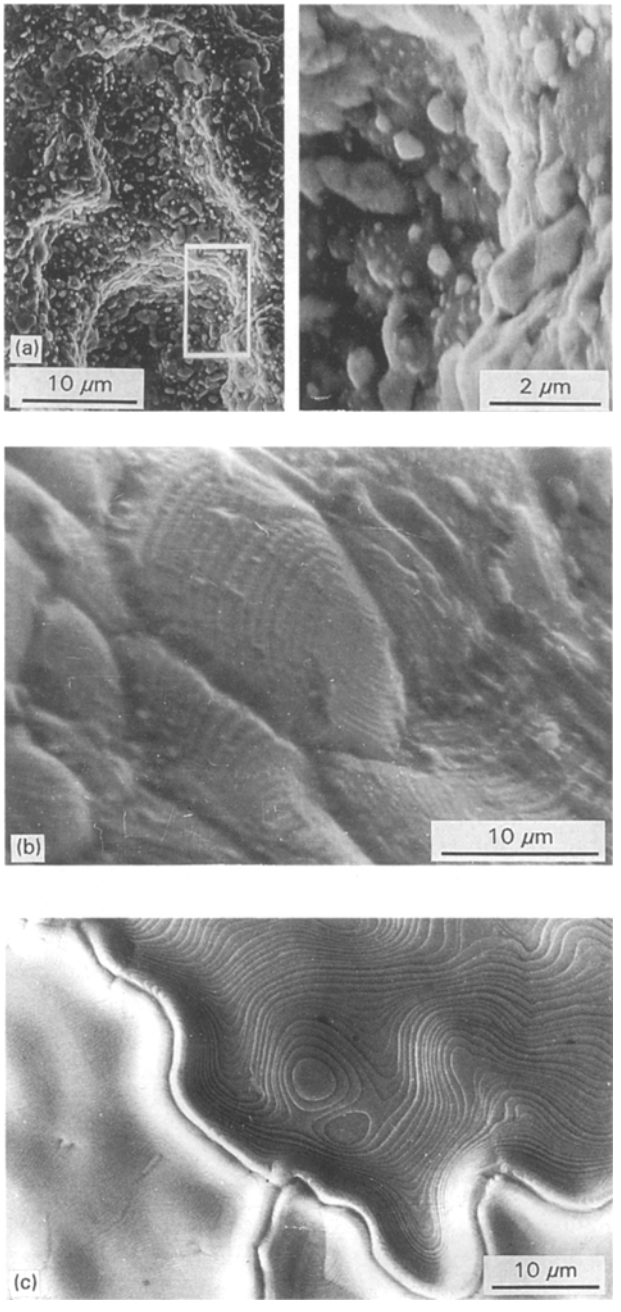

Figure 9 The morphology of the nickel-based layer deposited at 1520 K on to the KNT16 cermet: (a) the nucleation stage, (b, c) the merged nuclei.

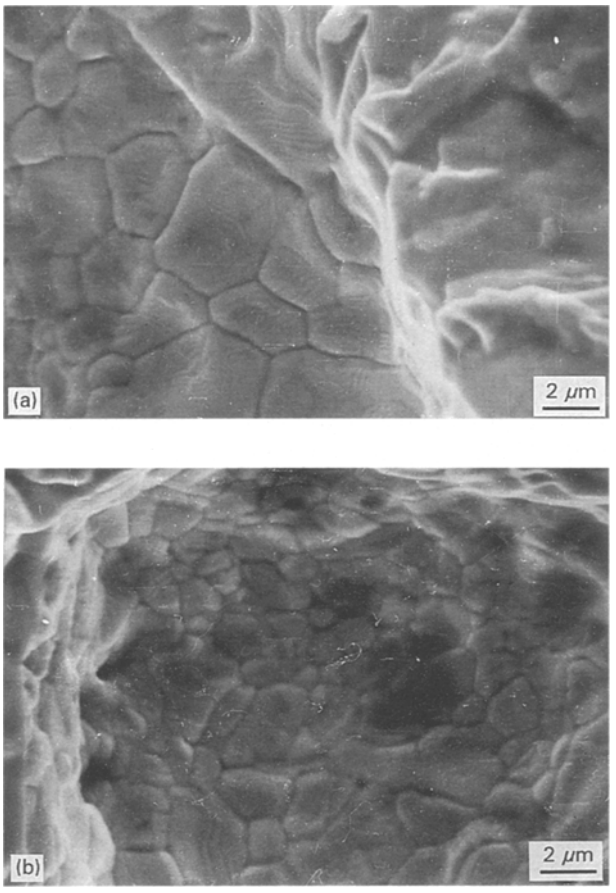

Figure 10 The morphology of the nickel-based layer deposited at different temperatures on the KNT16 cermet: (a) 1470 K, (b) 1420 K.

Ni–Cr layer, where the carbon mobility is highest, and the crystals have a ring-like structure in this stage (Fig. 11a). Then, the carbide coating grows out, becomes more and more irregular (Fig. 11b), and finally covers the entire surface of the Ni–Cr layer with a uniform sponge-like layer (Fig. 11c). The carbide layer seems to be porous; however, special electrochemical tests have revealed that the coating is absolutely pore-free.

Obviously, the sponge-like, irregular structure of the chromium carbide crystals is related to the fact that they supposedly grow from the Ni–Cr liquid-containing phase. Two processes, the external supply of chromium and internal supply of carbon, seem to define the carbide coating structure. In the case of the presence of a significant concentration gradient in a vapour phase between the growing crystal surface and the nearest distance from it, vapour-deposited coatings grow mainly perpendicular to the substrate surface. As a result, columnar or dendrite-like crystals are formed in this case and the same structure can obviously form in the case of the chromium carbide coating. However, because of some limiting factors connected with the diffusional supply of carbon from the substrate towards the top of the growing crystals and the presence of a liquid phase at the substrate surface, the carbide coating structure is more irregular.

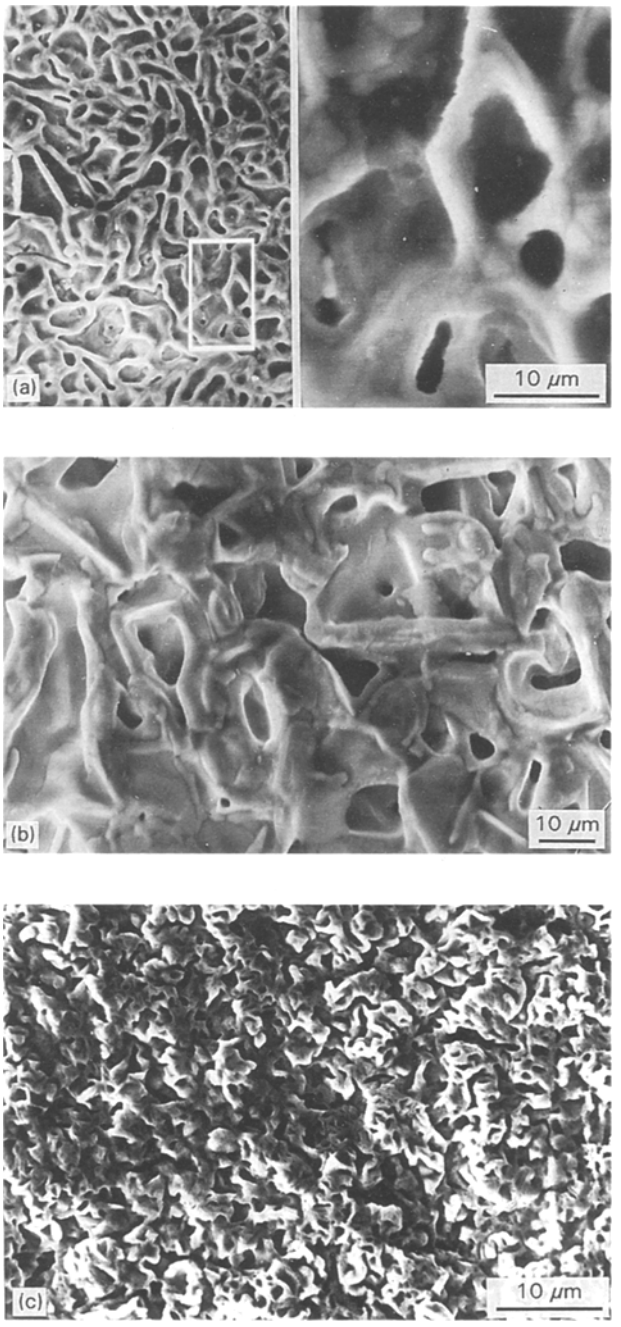

Figure 11 The morphology of the chromium carbide layer deposited on the KNT16 cermet at 1520 K: (a) the initial stage; (b, c) subsequent stages.

3.5. A possible mechanism, responsible for the interaction between the TiC- or TiCN-based cermets and chromium vapour

It is known that there are two triple eutectics in the Ni–Cr–C system (Fig. 12): the chromium-based E_1 (32% Ni, 67% Cr, 1% C) at 1270 °C and nickel based E_2 (76.5% Ni, 20% Cr, 3.5% C) at 1045 °C [17]. Meanwhile, it has been established that for the Cr_3C_2–Ni system, a liquid phase is never formed at the temperature of the E_2 eutectics (1045 °C) and a melting process takes place at a temperature between the E_2 and E_1 eutectic temperatures (approximately at 1180 °C) [16].

Obviously, when chromium vapour interacts with the cermets, a proportion of the concentrations of

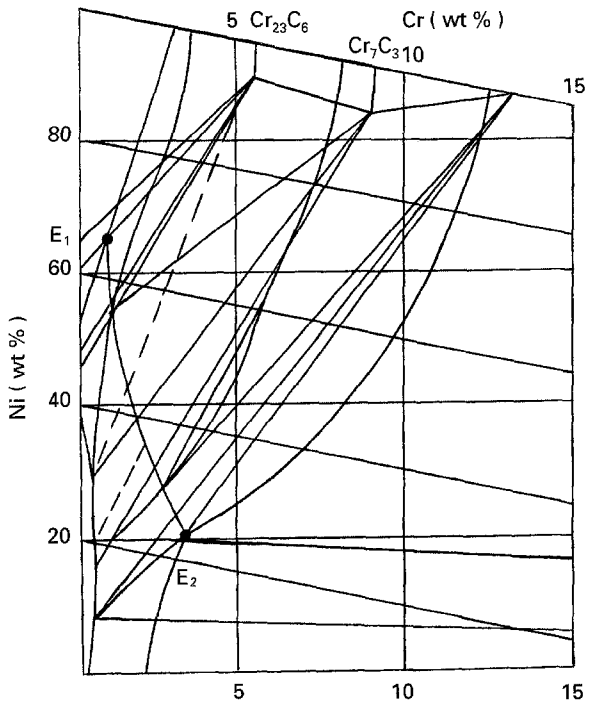

Figure 12 The equilibrium in the Ni–Cr–C system [17].

chromium, nickel and carbon can reach that corresponding to the E_2 eutectics. This seems to be possible because concentrations of nickel and chromium vary over a wide range with varying concentrations of chromium adsorbed on to the nickel-based binder surface, whereas the concentration of carbon dissolved in a nickel-based binder of cermets can reach several per cent [15] and, therefore, be close to 3.5% of the E_2 eutectics. It should be mentioned that the ratio between chromium and nickel in both the nickel-based underlayer (in the cases of the KNT16 and TN20 cermets) and nickel-based matrix of the coating (in the case of the model alloy) is quite close to that of the E_2 eutectics. Though the precision of measurement of carbon concentrations was not high enough, the carbon concentration in the nickel-based phase was estimated to reach 5 wt %, which was also close to that of the E_2 eutectics.

Thus, the mechanism of the interaction between the TiC(TiCN)–Ni–Mo hardmetals and chromium vapour can be described in the following way. The thermodynamic potential of the direct interaction between TiC (or TiCN) and chromium vapour is low and, in the case of the absence of a nickel-based binder, a chromium carbide coating cannot be formed due to the carbon contained in these refractory compounds. However, in the case of the presence of the nickel-based binder, a proportion of the concentrations of chromium, nickel and carbon reaches a value close to that of the nickel-based E_2 eutectics in the Cr–Ni–C system as a result of the adsorption of chromium at the surface of the nickel-based binder. This leads to the formation of a liquid phase at the substrate surface and chromium is deposited in the form of the Ni–Cr–C alloy, which is partly or fully liquid at the deposition temperature. In this case there is no slowing down of the deposition process in time connected with carbon diffusion from the substrate to the growing coating, and the process is described by linear kinetic curves. The Ni–Cr–C thin film covers all the substrate surface and crystallizes as the nickel-based interlayer after cooling.

When the Ni–Cr–C film reaches some definite thickness, obviously because of the limitations of carbon supply, further growth of this film can no longer occur because there is insufficient carbon for the formation of the liquid Ni–Cr–C phase. The chromium carbide-based coating close to the E_1 eutectics by composition, which is characterized by much lower carbon concentration compared to the E_2 eutectics, starts to grow under conditions of carbon shortage. Because this layer grows due to the carbon diffusion through the nickel-based film and the initially formed carbide film, carbon diffusion begins to hamper the deposition process and the kinetic curves are described by a parabolic dependence in this stage of the process. Nickel is continuously incorporated from the nickel-based interlayer into the carbide layer, and a mixture of $(Cr,Ni)_7C_3$ and $(Cr,Ni)_{23}C_6$ is formed instead of pure chromium carbides. Because the chromium carbide-based layer grows from the Ni–Cr–C liquid phase it is characterized by an irregular structure. In the case of substrates with high binder concentrations chromium carbides are formed as separated inclusions surrounded by the nickel-based matrix.

Nucleation of the carbide coating takes place by the grain boundaries of the Ni–Cr–C film and, initially, the carbide coating has a ring-like structure. Then, the carbide layer covers the entire surface of the nickel-based interlayer and the two-layer structure is formed on the cermets' surface.

It should be noted that though carbon diffusion through the initially formed interlayer is reflected in the shape of the kinetic curves, carbon diffusion is not a limiting stage of the deposition process according to the value of the activation energy obtained. The limiting stage of the deposition process, as a whole, is supposed to be the external chromium supply, which is connected with the rate of chromium evaporation. In this case, there is no noticeable diffusional decarbonization of the substrate, because carbon diffusion must supposedly occur at a rate higher than that of the coating growth.

4. Conclusion

The interaction between TiC(TiCN)–Ni–Mo cermets and chromium vapour leads to the formation of a two-layer coating. The coating includes an Ni–Cr–C interlayer 1–2 μm thick and a layer of a mixture of $(Cr,Ni)_7C_3$ and $(Cr,Ni)_{23}C_6$ 6–8 μm thick. The coating deposition process consists of the initial stage described by the linear dependence, and a subsequent stage described by the parabolic dependence. The value of the activation energy of the process is 387 kJ mol^{-1}, which is close to the heat of evaporation of chromium, and the chromium evaporation process is supposed to be a limiting stage of the deposition process as a whole. The coating nucleates as

"drops" of the Ni–Cr–C phase which then grow outwards, forming a continuous film. The carbide layer is initially deposited by the grain boundaries of the Ni–Cr–C coating in the form of a ring-like structure which then transforms to the coating with an uniform structure.

The proposed mechanism of the interaction between the cermets and chromium vapour phase includes an initial formation of a liquid phase by melting of the eutectics in the Ni–Cr–C system at a temperature of 1045 °C. The chromium carbide-based layer then crystallizes from the liquid phase as a result of the internal carbon diffusion and external chromium supply from the chromium vapour phase.

References

1. W. SHINTLMEISTER, O. PACHER K. PFFAFINGER and T. RAINE, *J. Electrochem. Soc.* **123** (1976) 924.
2. W. SHINTLMEISTER, O. PACHER, T. KRALL and T. RAINE, *Powder Metall. Int.* **13** (1981) 71.
3. T. LENSKAYA, V. TOROPCHENOV, A. ANIKEEV and T. MAMAEVA, "Manufacture and Application of Cemented Carbides" (Metallurgia, Moscow, 1982) p. 107.
4. O. ROMAN, L. KIRILUK and S. CHERNOUHOVA, *Sov. Powder Metall. Met. Ceram.* **6** (1987) 52.
5. K. BARTSCH, A. LEONARDT, E. WOLF, M. SCHONHERR and M. SEIDLER, *J. Mater. Sci.* **22** (1987) 3032.
6. I. KONYASHIN, YU. KOROLEV, A. ANIKEEV, A. KORCHAGIN and A. ZARAHKANI, "Proceedings of the 12th International Plansee Seminar", edited by H. Bildstein and H. Ortner, Reutee, Austria, Vol. 3 (Metallwerk Plansee, Reutee, 1989) p. 119.
7. I. FRANTSEVICH L. GAEVSKAYA and L. BELOBORODOV, *Powder Metall.* **5** (1983) 53.
8. Ja. MUSIKANT and V. SAMOILOV, "Cutting Tools with Cermets Inserts" (NIIMASH, Moscow, 1984).
9. V. KRUCHKOV, *Machines Tools* **7** (1987) 25.
10. M. KATO, H. YOSHIMURA and Y. FUJIWARA, in "Proceedings of the 12th International Plansee Seminar", Reutee, Austria, Vol. 3 (1989) p. 93.
11. I. KONYASHIN A. ZARAKHANI and E. LEONOV, *Non-Ferrous Metals* **5** (1988) 76.
12. S. BADRAK, T. BARTNITSKAYA and M. BARYSHEVSKAYA, *Powder Metall.* **9** (1981) 66.
13. J. GUNO and D. KOLAR, *J. Less-Common Metals* **31** (1973) 331.
14. K. MISHENKO and A. RAVDEL (eds), "Reference Book of Physical Chemistry" (Leningrad, 1974).
15. V TRETYAKOV, "Materials Science and Technology of Hardmetals" (Metallurgia, Moscow, 1976).
16. V. GRIGORYEVA and V. KLIMENKO, "Chromium Carbide Alloys" (Naukova Dumka, Kiev, 1961).
17. W. KOSTER *et al. Arch. Eisenhutten.* **10** (1955) 72.

Received 30 June 1994
and accepted 3 February 1995